Luminescent Soft Material: Two New Europium-Based Ionic Liquids

by **Sifu Tang**[a]), **Joanna Cybinska**[a])[b]), and **Anja-Verena Mudring***[a])

[a]) Anorganische Chemie I – Festkörperchemie und Materialien, Ruhr-Universität Bochum, D-44801, Bochum (e-mail: anja.mudring@rub.de)

[b]) Faculty of Chemistry, University of Wrocław, Joliot-Curie 14, PL-50-383 Wrocław

Dedicated to Professor Dr. *Jean-Claude Bünzli* on the occasion of his 65th birthday

Two new Eu-based ionic liquid systems, $[C_4mim][DTSA]:[Eu(DTSA)_3]$ and $2[C_4mim][DTSA]:[Eu(DTSA)_3]$ were synthesized at 120° under inert conditions from 1-butyl-1-methylimidazolium ditoluenesulfonylamide ($[C_4mim][DTSA]$). The identity and purity of the synthesized compounds were confirmed by elemental analysis, IR, *Raman*, and ^{1}H-NMR spectroscopy. As they solidify below 100° as glasses they qualify as ionic liquids. Fluorescence measurements show that the materials exhibit a strong red luminescence of high color purity. Therefore, they have the potential to be used for optical applications such as in emission displays.

Introduction. – In the past few years, ionic liquids (ILs) have attracted considerable attention due to their unique chemical and physical properties [1], such as low vapor pressure, wide liquid range, large electrochemical window, and so on. ILs are seen as 'multi-purpose liquids' and have already found usage in almost every field of chemistry (*e.g.* separation/extraction, catalysis, synthesis, electrochemistry) [2]. As commonly accepted, ionic liquids are organic salts, composed of distinct cations and anions which melt below 100°. When a metal ion is introduced into the complex anion of the ionic liquid, a so-called metal-containing ionic liquid is obtained. Compared to ordinary organic ionic liquids, metal-containing ionic liquids combine both the properties of ionic liquids and those of the metal cation which can be magnetic, photo physical/optical or catalytic properties [3]. Recently a row of investigations devoted to lanthanide-containing ionic liquids have shown that solutions of lanthanide compounds in ionic liquids are promising soft luminescent materials for use in photochemistry and spectroscopy [4–8]. It is very well-known that especially lanthanide (Ln) β-diketonate complex compounds exhibit very strong luminescence sensitized by efficient photon absorption in the organic ligand. Such a process, called 'antenna effect', involves the energy transfer of the absorbed photon to the triplet state of the ligand and subsequent intramolecular transfer to the Ln^{III} ion. As a consequence, enhancement in the Ln^{III} emission is observed. However, it is very important to notice that the efficiency of this process depends strongly on the donor–acceptor properties of the ligands which influence the energy of the charge transfer (CT) state, controlling the energy transfer and efficiency of Ln emission [9–13].

Ln-Containing ionic liquids can be obtained by two methods. The first method is to dissolve a Ln complex or oxide in an ionic liquid. A high quantum yield and an

enhanced photostability of such Ln-containing ionic liquids – or better Ln-doped ionic liquids – was observed, for example, when doping an europium β-diketonate complex into a imidazolium ionic liquid [5] or by dissolving europium oxide and an organic ligand into a task-specific ionic liquid bearing a carboxylic group [6]. The merit of this method is its easy feasibility. However, the structure of the optically active component, especially the local environment of the Ln^{III} ion, is most of the times unknown and makes a strategic improvement of the material difficult. In contrast, by reacting a Ln salt with an ionic liquid which shares the same counter anion as the used ionic liquid leads to the formation of a compound or solution where the Ln^{III} ion is solely coordinated by the common anion. The target compound can be tuned by reacting the salt with the ionic liquid at different molar ratios or selecting different cations and anions. In our previous work, we synthesized *via* this method three dysprosium-based ionic liquids $[C_6mim]_{5-x}[Dy(SCN)_{8-x}(H_2O)_x]$ ($x = 0-2$, $C_6mim = 1$-hexyl-3-methylimidazolium) from $[C_6mim]SCN$, KSCN, and $Dy(ClO_4)_3 \cdot 6\ H_2O$. These ILs show high response to external magnetic fields and have excellent photophysical properties [7]. Three Eu-containing ionic liquids with the compositions $[R]_x[Eu(Tf_2N)_{3+x}]$ ($Tf_2N =$ bis(trifluoromethanesulfonyl)amide; $x = 1$ for R = 1-propyl-3-methylimidazolium (C_3mim) and 1-butyl-3-methylimidazolium (C_4mim); $x = 2$ for R = 1-butyl-3-methylpyrrolidinium (C_4mpyr) were also obtained without the using of neutral co-ligands [8]. They show excellent photophysical properties such as long lifetimes of luminescence at high Eu^{III} concentration, small linewidth, and high color purity. To improve the photophysical properties, we continued our work by replacing the CF_3 groups of the Tf_2N anion with toluene groups in the ligand (DTSA = ditoluenesulfonylamide) in the hope that the toluene group can serve as a better light-absorbing chromophore (antenna).

Results and Discussion. – Materials with compositions similar to the Eu-Tf_2N compounds which we investigated previously [8], were studied. $[C_4mim][DTSA]:[Eu(DTSA)_3]$ and $2[C_4mim][DTSA]:[Eu(DTSA)_3]$ were synthesized at 120° under inert conditions from 1-butyl-3-methylimidazolium ditoluenesulfonylamide ($[C_4mim][DTSA]$) and europium ditoluenesulfonylamide ($Eu[DTSA]_3$).

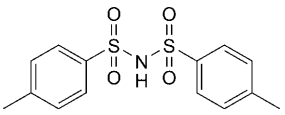

HDTSA

Thermal Properties. DSC (differential scanning calorimetry) shows that all materials qualify as ionic liquids as they solidify below 100° (*Fig. 1*). The DSC traces show a thermal behavior which is commonly encountered for ionic liquids: Crystallization is strongly inhibited and the compounds solidify rather as a glass. This also makes the determination of a reliable phase diagram impossible, and we cannot judge whether $[C_4mim][DTSA]:[Eu(DTSA)_3]$ and $2[C_4mim]_2[DTSA]:[Eu(DTSA)_3]$ are true compounds or have rather to be viewed as a solution of $[Eu(DTSA)_3]$ in $[C_4mim][DTSA]$.

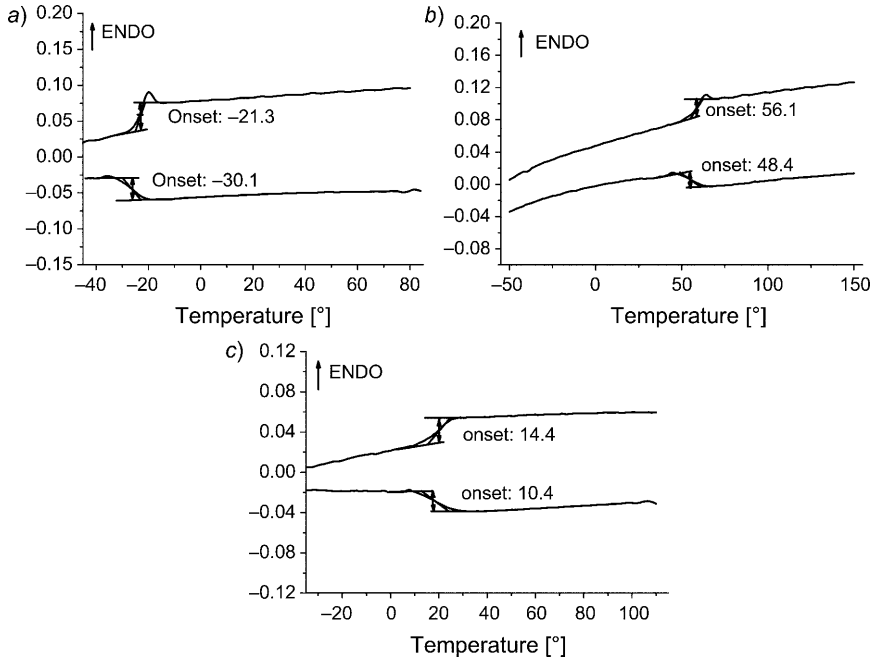

Fig. 1. *Thermogram of [C₄mim][DTSA] (a), [C₄mim][DTSA]:[Eu(DTSA)₃] (b), and 2[C₄mim]-[DTSA]:[Eu(DTSA)₃] (c)*

Structural Characterization. Unfortunately neither by employing homogeneous or heterogeneous crystallization techniques we were able to obtain crystalline materials in the system $[C_4mim][DTSA]/[Eu(DTSA)_3]$. In consequence, the materials were characterized by vibrational spectroscopy. *Fig. 2* shows a comparison of the infrared (IR) spectra of the materials, *Fig. 3* the respective *Raman* spectra.

The IR and *Raman* spectra provide good evidence that the metal ion is coordinated by the DTSA anion. For the 'free' $DTSA^-$ in the ionic liquid $[C_4mim][DTSA]$, the $\nu_s(SNS)$ band is found at 768 cm^{-1}. Under complexation, the $\nu_s(SNS)$ band of the anion shifts in $[C_4mim][DTSA]:[Eu(DTSA)_3]$ and $2[C_4mim][DTSA]:[Eu(DTSA)_3]$ to 774 and 772 cm^{-1}, respectively (see *Fig. 3*). The $\nu_s(SO_2)$ which should be directly influenced by coordination of the sulfonyl O-atom to a metal center is observed for the ionic liquid $[C_4mim][DTSA]$ at 1150 cm^{-1}. In $[C_4mim][DTSA]:[Eu(DTSA)_3]$ and $2[C_4mim]-[DTSA]:[Eu(DTSA)_3]$ this spectral region is broadened due to the overlap of S–O modes involving the coordinating and non-coordination sulfonyl O-atoms. The peaks are located at 1152 and 1162 cm^{-1}, respectively, indicating a weakening of the S–O bond upon coordination. A similar observation was made for alkaline earth-Tf_2N complexes [9] and for the above mentioned Eu(III)-Tf_2N ionic liquids [8]. It is highly likely that the first coordination shell around Eu^{III} in $[C_4mim][DTSA]:[Eu(DTSA)_3]$ and $2[C_4mim][DTSA]:[Eu(DTSA)_3]$ is similar to the one in $[C_4mim][Eu(Tf_2N)_4]$ where nine O-atoms form an irregular coordination polyhedron around Eu^{III}, which can be best described as a strongly distorted monocapped square anti-prism.

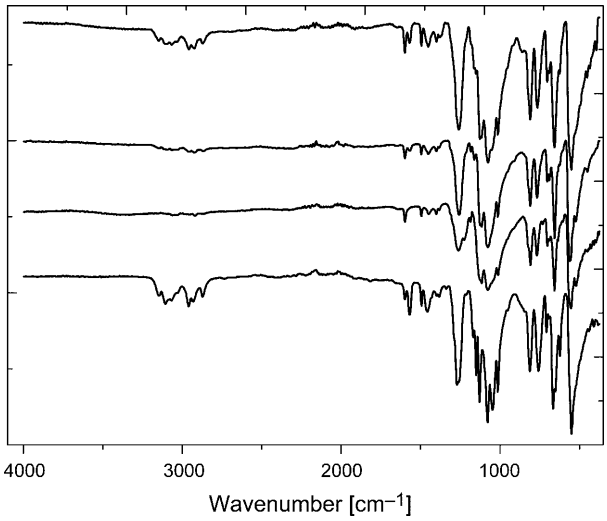

Fig. 2. *IR Spectra of, from top to bottom, [C4mim][DTSA], Eu[DTSA]3, [C4mim][DTSA]:[Eu(DTSA)3], and 2[C4mim][DTSA]:[Eu(DTSA)3]*

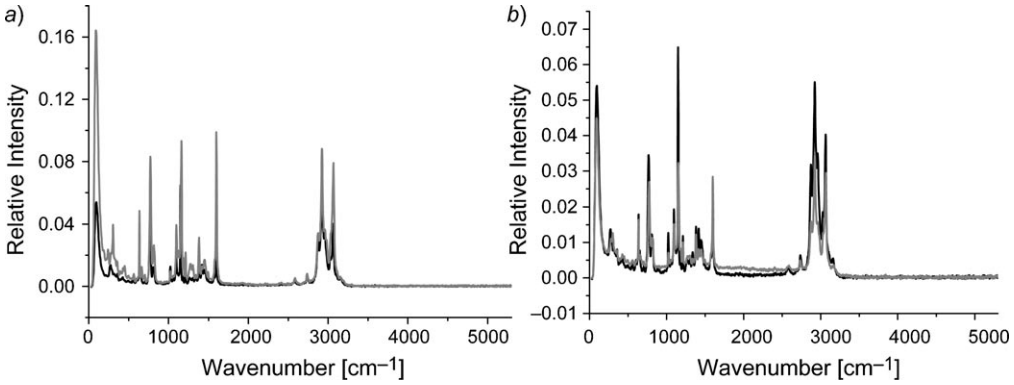

Fig. 3. *a*) *Comparison of the* Raman *spectra of [C4mim][DTSA]* (black) *and [C4mim][DTSA]:[Eu(DTSA)3]* (grey) *and b*) *[C4mim][DTSA]* (black) *and 2[C4mim][DTSA]:[Eu(DTSA)3]* (grey)

Photophysical Properties. The excitation ($\lambda_{ex} = 393$ nm and $\lambda_{ex} = 290$ nm) and emission ($\lambda_{em} = 615$ nm) spectra of $Eu[DTSA]_3$, $[C_4mim][DTSA]:[Eu(DTSA)_3]$, and $2[C_4mim][DTSA]:[Eu(DTSA)_3]$ were recorded at three different temperatures, namely 77, 298 and 353 K (*Figs. 4–6*). The results show that the respective spectra are quite similar and all show the characteristic Eu^{III} f–f-transitions.

For the reason that the excitation and emission of $[C_4mim][DTSA]:[Eu(DTSA)_3]$ and $2[C_4mim][DTSA]:[Eu(DTSA)_3]$ show no significant deviations, we will discuss and compare only the data obtained for $Eu[DTSA]_3$ and $[C_4mim][DTSA]:[Eu(DTSA)_3]$. The excitation spectrum of the samples recorded at liquid N_2 temperature, under

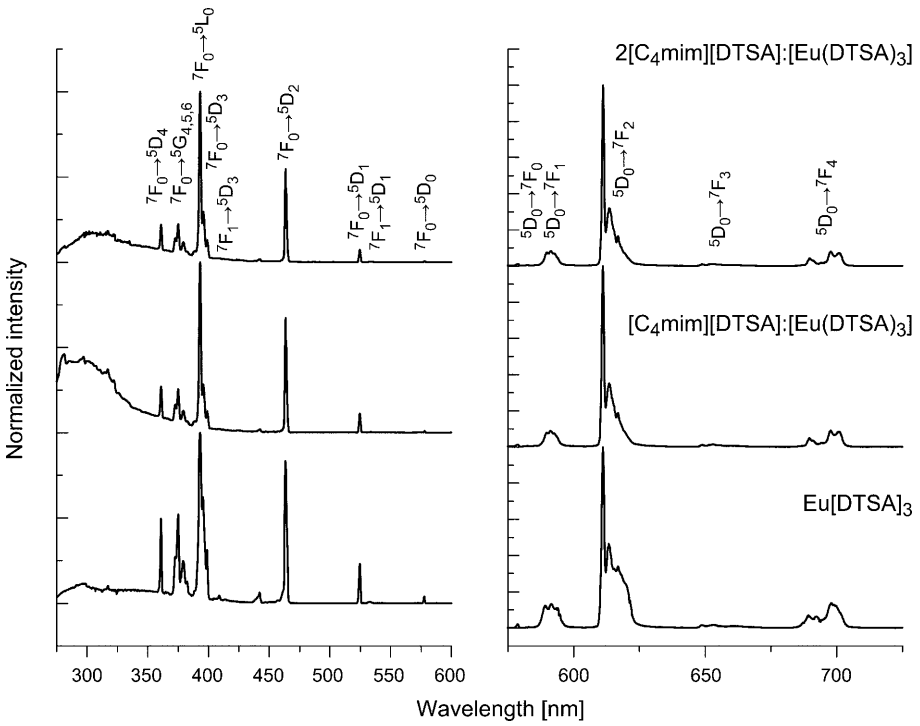

Fig. 4. *a*) *Excitation and b*) *emission spectra of Eu[DTSA]$_3$, [C$_4$mim][DTSA]:[Eu(DTSA)$_3$], and 2[C$_4$mim][DTSA]:[Eu(DTSA)$_3$], recorded at 77 K*

emission of the $^5D_0 \rightarrow {}^7F_2$ transition at $\lambda_{em} = 611$ nm, show a broad band between 250 and 320 nm attributed to $\pi-\pi^*$ transitions of the DTSA ligand. The narrow, much more intense lines in the spectrum correspond to discrete f–f transitions at 360.5, 365 ($^7F_0 \rightarrow {}^5D_4$), 372, 375 ($^7F_{0/1} \rightarrow {}^5G_J$), 379, 383 ($^7F_{0/1} \rightarrow {}^5L_7$, ^5G_J), 392.5, 395 ($^7F_0 \rightarrow {}^5L_6$), 414.5 ($^7F_0 \rightarrow {}^5D_3$), 463 ($^7F_0 \rightarrow {}^5D_2$), 524 ($^7F_0 \rightarrow {}^5D_1$), and 534 nm ($^7F_1 \rightarrow {}^5D_1$). The presence of a broad band in the UV region proves that the DTSA ligand transfers the absorbed photons to Eu(III). The maximum of this broad band is found at comparatively high energies (*ca.* 290 nm). Ligand singlet states can serve as a donating state in the sensitization of, for example, Eu^{III} and Sm^{III} ions, however usually excited states of luminescent Ln^{III} ions are populated by a fast intramolecular energy transfer process from a triplet state of the ligand. The ligand triplet state is populated from the singlet state by intersystem crossing [10][14].

At low temperature (77 K), the intensity of the ligand band compared to the narrow Eu^{III} transitions is not very high, which suggests a low efficiency in the energy transfer process. For [C$_4$mim][DTSA]:[Eu(DTSA)$_3$], the intensity of this broad band drastically decreases with rising the temperature to 353 K, only narrow lines attributed to Eu^{III} f–f transitions can be observed. The decrease of the efficiency of energy transfer with decreasing temperature is probably due to the fact that the CT state is

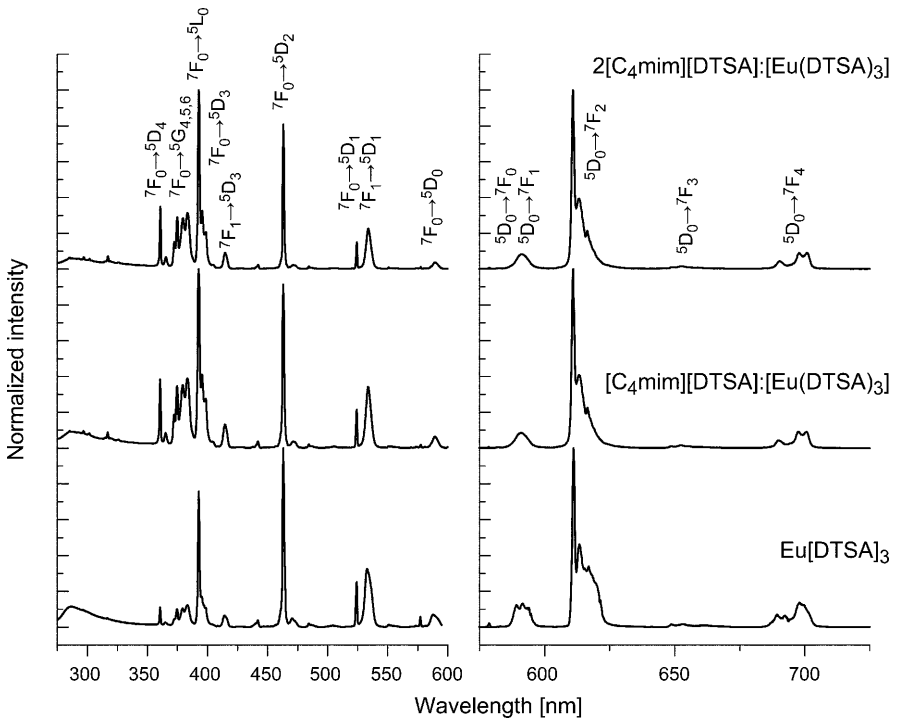

Fig. 5. *a*) *Excitation and b*) *emission spectra of Eu[DTSA]$_3$, [C$_4$mim][DTSA]:[Eu(DTSA)$_3$], and 2[C$_4$mim][DTSA]:[Eu(DTSA)$_3$] recorded at 298 K.*

involved in the de-activation process. Such an effect was already noted for several Eu^{III} complexes [14][15].

Analysis of low-temperature excitation spectra indicates that some of these lines may be accompanied by a number of satellites of vibronic or ion pair origin. Sharp lines in the excitation spectra recorded at room temperature are associated with transition from the ground-state ($^7F_0$) and also from the first excited state ($^7F_1$) of the Eu^{III} ion to different ^5D_J states, according to the thermal population of $^7F_{1,2}$ levels of the Eu^{III} ion. This assumption is backed by the higher intensity of the $^7F_1 \rightarrow {}^5D_1$ transition at elevated temperature (353 K).

The luminescence spectra recorded at the three different temperatures (77, 298, and 353 K) under excitation into the band corresponding to the $^7F_0 \rightarrow {}^5L_6$ transition of the Eu^{III} ion ($\lambda_{ex} = 393$ nm) all show a strong red light emission. The spectra consist of sharp lines attributed to $^5D_0 \rightarrow {}^7F_J$ ($J = 0-4$) transitions of Eu^{III} (578.5 ($^5D_0 \rightarrow {}^7F_0$), 591 ($^5D_0 \rightarrow {}^7F_1$), 611, 613.5, 616.5 ($^5D_0 \rightarrow {}^7F_2$), 653 ($^5D_0 \rightarrow {}^7F_3$) and 690, 698 nm ($^5D_0 \rightarrow {}^7F_4$). The spectra are dominated by a band with a maximum around 611 nm which belongs to the hypersensitive transition $^5D_0 \rightarrow {}^7F_2$ in agreement with a low point symmetry for Eu(III). Although the emission occurs mainly from the $^5D_0$ level, it is important to note that also transitions from the higher energy $^5D_1$ level can be observed in the spectral range from 520 to 570 nm. Neither Eu(DTSA)$_3$ nor [C$_4$mim][DTSA]:[Eu(DTSA)$_3$]

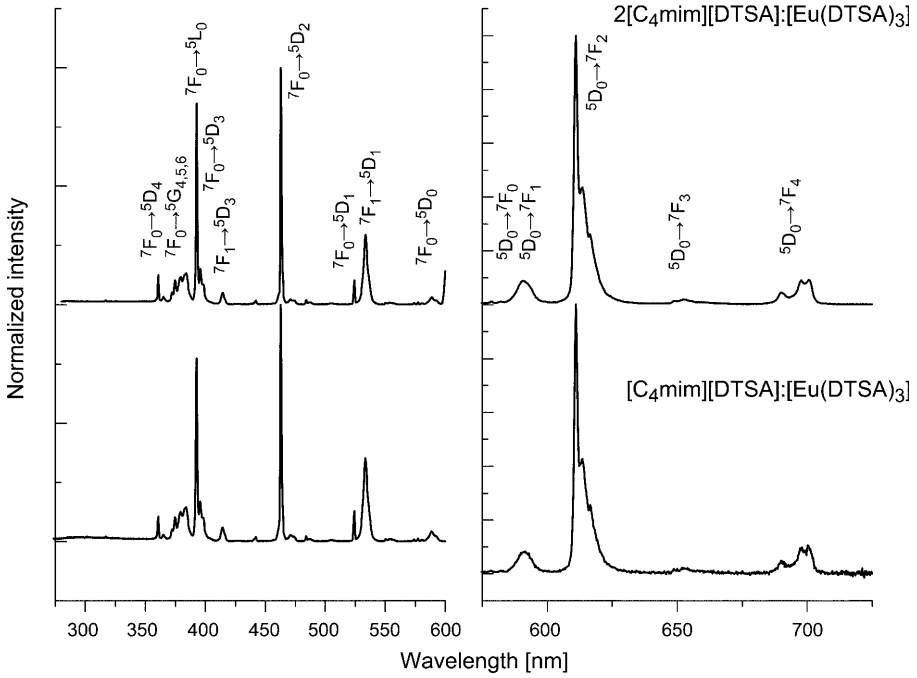

Fig. 6. *a*) *Excitation and b*) *emission spectra of [C4mim][DTSA]:[Eu(DTSA)3], and 2[C4mim]-[DTSA]:[Eu(DTSA)3] recorded at 353 K.*

are sensitive to changes in the energy of excitation. The emission spectra recorded under excitation into UV and directly into the Eu^{III} levels are the same in sense that, the shapes of the band as well as their relative intensities are not changing. The bands assigned to the $^5D_0 \rightarrow {}^7F_J$ ($J = 0-4$) transitions are relatively broad and unsplitted. Lowering of the temperature does not lead to substantial band narrowing. The $^5D_0 \rightarrow {}^7F_0$ transition is unsplitted, however, relatively broad. The half width of the $^5D_0 \rightarrow {}^7F_0$ band is about 25 cm^{-1}. This could be due to a high flexibility in the local Eu^{III} surrounding. The decay rates can be fitted as monoexpontential curves, and all data collected in the *Table* were obtained in this way. For all samples, the decay times are strongly temperature dependent. At 298 K for $Eu(DTSA)_3$ the shortest decay time was obtained. This could confirm the assumption that the multiphonon relaxation processes for Eu^{III} in the IL are reduced because of better shielding. The relative intensities between the $^5D_0 \rightarrow {}^7F_2/{}^5D_0 \rightarrow {}^7F_1$ transitions can be used to determine the symmetry and strength of the ligand field around Eu^{III}. A variation of the ligand field strength leads to a change of the intensity of the electric dipole (ED) $^5D_0 \rightarrow {}^7F_2$ transition, in contrast to the intensity of the magnetic dipole (MD) $^5D_0 \rightarrow {}^7F_1$. The latter is hardly affected by the ligand field. In the systems under investigation the ratio is strongly temperature dependent. For $Eu(DTSA)_3$ at r.t. and 77 K, it is 9.7 and 7.6, respectively. For the $[C_4mim][DTSA]:[Eu(DTSA)_3]$ the asymmetry parameter vary with temperature between 11.2 (77 K), 11.7 (298 K), and 12 (353 K). The large ratio of the fluorescence intensities is typical for Eu^{III} in a low site symmetry without an inversion

center [16]. In the previously reported $[C_4mim][Eu(Tf_2N)_4]$, these values were equal to 8.36 and 3.49 for solid (crystalline) and liquid, respectively, which suggests larger Eu-ligand interaction in the solid compounds than in the liquids [8]. In the materials investigated here, the asymmetry parameter is higher and increasing with the temperature, indicating a stronger coupling between the anion and Eu^{III}, which can be expected at higher temperature [17].

Table. *Experimental Lifetime, Calculated Radiative and Nonradiative Decay Rates, and Quantum Efficiency* (q) *of the* $^5D_0$ *State for Eu[DTSA]$_3$ at 77 K and Room Temperature for [C$_4$mim][DTSA]:[Eu(DTSA)$_3$] at 77 K, Room Temperature, and 353 K, as well as for 2[C$_4$mim][DTSA]:[Eu(DTSA)$_3$] at 77 K, Room Temperature, and 353 K*

Compounds	Temp. [K]	τ [ms]	k_r	k_{nr}	q [%]
$Eu[DTSA]_3$	77	1.67	0.35	0.248	58.5
$Eu[DTSA]_3$	298	1.24	0.44	0.366	54.6
$[C_4mim][DTSA]:[Eu(DTSA)_3]$	77	1.88	0.39	0.142	73.3
$[C_4mim][DTSA]:[Eu(DTSA)_3]$	298	1.608	0.44	0.182	70.8
$[C_4mim][DTSA]:[Eu(DTSA)_3]$	353	1.20	0.42	0.413	50.4
$2[C_4mim][DTSA]:[Eu(DTSA)_3]$	77	1.84	0.39	0.153	71.8
$2[C_4mim][DTSA]:[Eu(DTSA)_3]$	298	1.615	0.43	0.189	69.5
$2[C_4mim][DTSA]:[Eu(DTSA)_3]$	353	1.13	0.40	0.485	45.2

To characterize the luminescence of $Eu(DTSA)_3$, $[C_4mim][DTSA]:[Eu(DTSA)_3]$, and $2[C_4mim][DTSA]:[Eu(DTSA)_3]$ with respect to its emission color under excitation 366 nm at 77, 293, and 353 K, the CIE (x,y) coordinates were calculated (*Fig. 7*). As it could be seen from the excitation spectra recorded at $^5D \rightarrow {}^7F_2$ transition, the imidazolium states are involved into energy transfer to Eu(III). However, it is very well known, that UV light induces transitions in the imidazolium ring and as consequence one can observe a broad emission band in the 400–600 nm spectral range [17]. Using the line 366 nm we were able to simultaneously excite the imidazolium ring and the Eu^{III} ions. In consequence, we observed a change of color of emission depending on the number of imidazolium groups present in the material. As it could be expected, a pure red color was obtained for the $Eu(DTSA)_3$. For the other materials, the color was shifted to blue due to contributions of imidazolium emission. It is also important to notice, that only for $Eu(DTSA)_3$ the color is almost temperature independent.

To check if the quantum yield depends on the first coordination shell of Eu^{3+} and temperature, we tried to estimate the $^5D_0$ quantum efficiency (q) from the emission spectrum and lifetime of the $^5D_0$ state by assuming that only nonradiative (k_{nr}) and radiative (k_r) processes are involved in the depopulation of the $^5D_0$ state [18]. The q can be defined as:

$$q = k_r/(k_r + k_{nr}) \quad (1)$$

The influence of the $^5D_0 \rightarrow {}^7F_{5,6}$ transitions on the depopulation of the $^5D_0$ state can be ignored because of their relatively weak intensities with respect to those of the remaining $^5D_0 \rightarrow {}^7F_{0-4}$ transitions [19]. The radiative contribution therefore can be

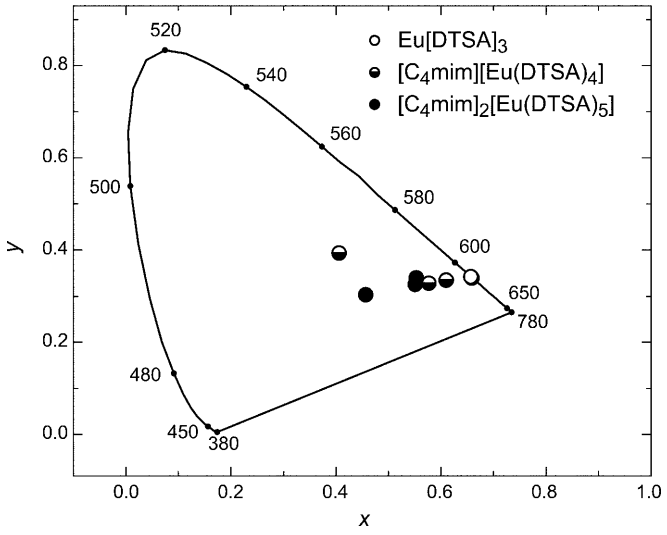

Fig. 7. *CIE Color coordinates for Eu[DTSA]$_3$, [C$_4$mim][DTSA]:[Eu(DTSA)$_3$], and 2[C$_4$mim]-[DTSA]:[Eu(DTSA)$_3$] at 77, 298, and 353 K*

calculated from the relative intensities of the $^5D_0 \rightarrow {}^7F_{0-4}$ transitions and can be expressed as:

$$k_r = A_{0\rightarrow1} \frac{\hbar\omega_{0\rightarrow1}}{S_{0\rightarrow1}} \sum_{J=0}^{4} \frac{S_{0-J}}{\hbar\omega_{0\rightarrow1}} \tag{2}$$

where $A_{0\rightarrow1}$ is the *Einstein* coefficient of spontaneous emission between the $^5D_0$ and $^7F_1$ *Stark* levels, usually considered to be equal to 50 s^{-1}. The $\hbar\omega_{0\rightarrow J}$ and $S_{0\rightarrow J}$ are the energy and the integrated intensity of the $^5D_0 \rightarrow {}^7F_J$ transitions, respectively. Appropriate analyses of the emission spectra of [C$_4$mim][DTSA]:[Eu(DTSA)$_3$] yielded the quantum efficiencies to be 0.733 (77 K), 0.708 (298 K), and 0.504 (353 K) (for 2[C$_4$mim][DTSA]:[Eu(DTSA)$_3$] these numbers were 77 K: 0.718, 298 K: 0.695, 353 K: 0.452) (see *Table*). It is obvious that the compounds have the highest quantum efficiency at 77 K and the lowest at 353 K. The lower value (50.4%) at higher temperature is caused by the higher nonradiative transition probability (k_{nr}), but when compared with those of some europium bistriflimide complexes Eu[N(SO$_2$C$_3$F$_7$)$_3$] (5%) or Eu[N(SO$_2$C$_3$F$_7$)$_3$][L]$_8$ (L = DPSO, diphenyl sulfoxide, 32%; L = TPPO, triphenylphosphine oxide, 5.6%; L = phen, phenanthroline, 5.1%) (0.05 mol/l MeCN solution) [20], this number is still very high, especially when the high Eu^{III} concentration is considered.

Conclusions. – In summary, two Eu-based ionic liquids have been synthesized. The identity and purity of the synthesized compounds were confirmed by elemental analysis, IR, *Raman* and ^{1}H-NMR spectroscopy. Their thermal behaviour was investigated by DSC. Both compounds, [C$_4$mim][DTSA]:[Eu(DTSA)$_3$] and 2[C$_4$mim][DTSA]:[Eu(DTSA)$_3$], qualify as ionic liquids as they solidify well below

100°, 2[C_4mim][DTSA]:[Eu(DTSA)$_3$] even below room temperature. However, no crystallization could be observed – only glass formation. [C_4mim][DTSA]:[Eu(DTSA)$_3$] and 2[C_4mim][DTSA]:[Eu(DTSA)$_3$] exhibit a bright red luminescence of high color purity. Therefore, they have the potential to be used in optical applications such as in emission displays. Further work will be undertaken to the synthesis of luminescent ionic liquids by the replacement of C–H bonds by electron-withdrawing C–F bonds in the chelating parts of the ligands to tune the LMCT states as well as minimize the non-radiative decay pathways.

Support by the DFG priority program SPP 1191 'Ionic Liquids' and the Fonds der Chemischen Industrie through a Dozentenstipendium for *A.V.M.* is gratefully acknowledged.

Experimental Part

Instrumentation. IR Spectra: *Bruker Alpha-P* FT-IR spectrometer in the range of 4000–400 cm^{-1}. *Raman* Spectra: from the bulk solids recorded at 150 mW on a *Bruker IFS-FRA-106/s*; for the measurement, the respective samples were sealed under Ar atmosphere in glass capillaries; the data were recorded at r.t. ^{1}H-NMR Spectra: *Bruker Advance DPX-250* instrument. Elemental analyses: *Vario EL III* elemental analyzer. Phase transition temperatures: differential scanning calorimeter (*NETZSCH DSC 240 F1*); measurements were carried out at a heating rate of 5°/min and an Ar flow rate of 20 ml/min; the reference sample was an empty Al container; the measurements with *ca.* 10 mg of [C_4mim][DTSA]:[Eu(DTSA)$_3$] and 2[C_4mim][DTSA]:[Eu(DTSA)$_3$] were performed under Ar in cold-sealed aluminium containers. Immediately before the measurement the Al lid was pierced to allow for the thermal expansion of Ar. Solid state excitation and emission spectra were recorded using a *Fluorolog 3* (*Jobin Yvon GmbH*, München, Germany) with a Xe lamp as the excitation source and a photomultiplier tube for detection; bulk samples were sealed in silica cells (1 cm). Electronic transitions were assigned according to the energy level diagrams of trivalent rare earth ions [21].

Synthesis of [C$_4$mim][DTSA]. Equal molar amounts of 1-butyl-3-methyl-1*H*-imidazol-1-ium chloride ([C_4mim]Cl) and sodium bis[4-methylphenyl)sulfonyl]azanide (Na[DTSA]) were dissolved in dry acetone, the soln. was stirred for 24 h at 80°. Then, the white precipitate was filtered off and the solvent was removed by using a rotary evaporator. The obtained viscous liquid was dried for 48 h at 60°. IR: 3147.3*w*, 3105.9*w*, 3067.3*w*, 2960.1*m*, 2930.1*w*, 287*w*, 1598.9*w*, 1568.9*m*, 1496.0*w*, 1457.4*m*, 1270.3*s*, 1150.3*s*, 1128.9*s*, 1077.4v*s*, 1047.4*s*, 1013.1*s*, 811.7*m*, 757.4*m*, 707.4*m*, 666.0*s*, 550.3v*s*. *Raman:* 95.1, 272.5, 359.3, 637.0, 768.2, 806.7, 1022.7, 1057.4, 1096.0, 1115.3, 1150.0, 1180.9, 1211.7, 1261.9, 1304.3, 1339.0, 1381.4, 1418.1, 1447.0, 1495.2, 1576.2, 1599.4, 2577.1, 2735.2, 2872.2, 2922.3, 2960.9, 3026.5, 3063.1. ^{1}H-NMR ($CDCl_3$, 250 MHz, 25°): 0.91 (*t*, *J* = 14.5, *Me*–CH_2); 1.30 (*sext.*, *J* = 37.3, Me–C*H*$_2$); 1.79–1.85 (*m*, Me–CH_2–C*H*$_2$); 2.29 (*s*, 2 *Me*–Ph); 4.03 (*s*, *Me*N); 4.27 (*t*, *J* = 14.8, CH_2–N); 6.98 (*d*, *J* = 9.3, 4 arom. H *ortho* to CMe); 7.25 (*s*, C*H*=CH); 7.35 (*s*, C*H*=CH); 7.51 (*d*, *J* = 8.0, 4 arom. H *ortho* to C–S); 9.66 (*s*, H–C(2) of imidazol). Anal. calc. for [C_4mim][DTSA] ($C_{22}H_{29}N_3O_4S_2$, 463.61): C 56.99, H 6.30, N 9.06, S 13.83; found: C 57.05, H 6.22, N 9.05, S 13.88.

Eu[DTSA]$_3$. The title compound was obtained by dissolving a slight excess of europium oxide in aq. soln. of 4-methyl-*N*-[(4-methylphenyl)sulfonyl]benzenesulfonamide, filtration of traces of non-reacted starting materials, and removal of the solvent. The obtained white solid was dried at 100° for 48 h in vacuum. IR: 1597.9*w*, 1494.7*w*, 1449.3*w*, 1401.6*w*, 1380.3*w*, 1260.4 (sh, *m*), 1224.7*m*, 1186.1*w*, 1115.7*s*, 1077.1v*s*, 1012.9*s*, 808.6*s*, 767.1*m*, 701.4*m*, 657.1*s*, 552.9v*s*, 521.4*s*. Anal. calc. for Eu(DTSA)$_3$ ($C_{42}H_{42}EuN_3O_{12}S_6$, 1125.1644): C 44.83, H 3.76, N 3.73, S 17.10; found: C 44.68, H 3.45, N 3.69, S 17.11.

Syntheses of [C$_4$mim][DTSA]:[Eu(DTSA)$_3$] and 2[C$_4$mim][DTSA]:[Eu(DTSA)$_3$]. In a small *Schlenk* tube, equal molar amounts of [C_4mim][DTSA] and Eu[DTSA]$_3$ (for 2[C_4mim][DTSA]:[Eu(DTSA)$_3$] the molar ratio was 2:1) were mixed and stirred at 120° for 2 h. Then the homogenous soln. was cooled to r.t. slowly.

Data of [C$_4$mim][DTSA]:[Eu(DTSA)$_3$]. IR: 3148.0v*w*, 3092.7v*w*, 3065.3v*w*, 2957.1v*w*, 2922.6v*w*, 2868.1v*w*, 1598.1*w*, 1568.7v*w*, 1495.0*w*, 1450.4*w*, 1400.7*w*, 1258.6*s*, 1116.0*s*, 1076.0v*s*, 1013.1*s*, 808.9*s*, 766.0*s*,

702.7*m*, 689.9*m*, 655.6v*s*, 559.1v*s*, 522.0 (sh, s). *Raman:* 89.3, 241.7, 303.4, 357.4, 428.8, 450.0, 563.8, 603.1, 662.1, 704.5, 772.0, 814.5, 1022.7, 1057.4, 1097.9, 1119.2, 1161.6, 1184.7, 1213.7, 1277.3, 1306.2, 1339.0, 1381.4, 1450.9, 1495.2, 1599.4, 2737.2, 2874.1, 2922.3, 2959.0, 2982.1, 3067.0. Anal. calc. for $[C_4mim][DTSA]:[Eu(DTSA)_3]$ ($C_{64}H_{71}EuN_6O_{16}S_8$, 1588.7863): C 48.38, H 4.50, N 5.29, S 16.15; found: C 48.40, H 4.66, N 5.55, S 15.85.

Data of 2 [C₄mim][DTSA]:[Eu(DTSA)₃]. IR: 3148.1v*w*, 3109.6v*w*, 3068.1v*w*, 2956.7v*w*, 2923.9v*w*, 2872.4v*w*, 1597.9*m*, 1569.3*w*, 1494.4*w*, 1451.6*w*, 1400.1*w*, 1380.1*w*, 1259.0*s*, 1126.1*s*, 1076.1v*s*, 1013.3*s*, 810.4*s*, 764.7*s*, 703.3*m*, 659.0*s*, 550.6v*s*. *Raman:* 93.2, 239.8, 276.4, 301.5, 357.4, 426.8, 448.0, 492.4, 558.0, 635.1, 658.2, 704.5, 774.0, 814.5, 1022.7, 1096.0, 1151.9, 1182.8, 1211.7, 1271.5, 1285.0, 1302.4, 1339.0, 1381.4, 1416.2, 1450.9, 1495.2, 1599.4, 2735.2, 2874.1, 2924.2, 2959.0, 3067.0. Anal. calc. for 2 $[C_4mim][DTSA]:[Eu(DTSA)_3]$ ($C_{86}H_{100}EuN_9O_{20}S_{10}$, 2052.4083): C 50.33, H 4.91, N 6.14, S 15.62; found: C 49.82, H 5.05, N 6.21, S 15.05.

REFERENCES

[1] N. V. Plechkova, K. R. Seddon, *Chem. Soc. Rev.* **2008**, *37*, 123.

[2] P. Wasserscheid, T. Welton, 'Ionic Liquids in Synthesis', Wiley-VCH, Weinheim, 2003; J. L. Anderson, J. Ding, T. Welton, D. W. Armstrong, *J. Am. Chem. Soc.* **2002**, *124*, 14247; V. Znamenskiy, M. N. Kobrak, *J. Phys. Chem. B* **2004**, *108*, 1072; S. V. Dzyuba, R. A. Bartsch, *Tetrahedron Lett.* **2002**, *43*, 4657; S. N. V. K. Aki, J. F. Brennecke, A. Samanta, *Chem. Commun.* **2001**, 413; A. J. Carmichael, K. R. Seddon, *J. Phys. Org. Chem.* **2000**, *13*, 591.

[3] P. Nockemann, B. Thijs, N. Postelmans, K. Van Hecke, L. Van Meervelt, K. Binnemans, *J. Am. Chem. Soc.* **2006**, *128*, 13658.

[4] a) K. Driesen, P. Nockemann, K. Binnemans, *Chem. Phys. Lett.* **2004**, *395*, 306; b) E. Guillet, D. Imbert, R. Scopelliti, J.-C. G. Bünzli, *Chem. Mater.* **2004**, *16*, 4063; c) A. Babai, A.-V. Mudring, *Chem. Mater.* **2005**, *17*, 6230; d) S. Arenz, A. Babai, K. Binnemans, K. Driesen, R. Giernoth, A.-V. Mudring, P. Nockemann, *Chem. Phys. Lett.* **2005**, *402*, 75.

[5] P. Nockemann, E. Beurer, K. Driesen, R. Van Deun, K. Van Hecke, L. Van Meervelt, K. Binnemans, *Chem. Commun.* **2005**, 4354.

[6] H. Li, H. Shao, Y. Wang, D. Qin, B. Liu, W. Zhang, W. Yan, *Chem. Commun.* **2008**, 5209.

[7] B. Mallick, B. Balke, C. Felser, A.-V. Mudring, *Angew. Chem.* **2008**, *120*, 7747; B. Mallick, B. Balke, C. Felser, A.-V. Mudring, *Angew. Chem., Int. Ed.* **2008**, *47*, 7635.

[8] S. Tang, A. Babai, A.-V. Mudring, *Angew. Chem.* **2008**, *120*, 7743; S. Tang, A. Babai, A.-V. Mudring, *Angew. Chem., Int. Ed.* **2008**, *47*, 7631.

[9] A. Babai, A.-V. Mudring, *Inorg. Chem.* **2006**, *45*, 3249.

[10] J.-C. G. Bünzli, 'Luminescent Lanthanide Probes as Diagnostic and Therapeutic Tools', in 'Metal Complexes in Tumor Diagnosis and as Anticancer Agents', Eds. A. Sigel, H. Sigel, Dekker, New York, 2004, Vol. 42, Chapter 2, pp. 39 – 75.

[11] G. F. de Sá, O. L. Malta, C. de Mello Donegá, A. M. Simas, R. L. Longo, P. A. Santa-Cruz, E. F. da Silva Jr., *Coord. Chem. Rev.* **2000**, *196*, 165.

[12] P. Gawryszewska, J. Sokolnicki, J. Legendziewicz, *Coord. Chem. Rev.* **2005**, *249*, 2489.

[13] J.-C. G. Bünzli, S. Comby, A.-S. Chauvin, C. D. B. Vandevyver, *J. Rare Earths* **2007**, *25*, 257.

[14] F. R. Goncalves e Silva, O. L. Malta, C. Reinhard, H. U. Güdel, C. Piguet, J. E. Moser, J.-C. G. Bünzli, *J. Phys. Chem. A* **2002**, *106*, 1670.

[15] P. Gawryszewska, O. L. Malta, R. L. Longo, F. R. Goncalves e Silva, S. Alves Jr., K. Mierzwicki, Z. Latajka, M. Pietraszkiewicz, J. Legendziewicz, *ChemPhysChem* **2004**, *5*, 1577.

[16] L. S. Fu, R. A. Sá Ferreira, N. J. O. Silva, A. J. Fernandes, P. Ribeiro-Claro, I. S. Gonçalves, V. De Zea Bermudez, L. D. Carlos, *J. Mater. Chem.* **2005**, *15*, 3117; K. Binnemans, P. Lenaerts, K. Driesen, Christiane Görller-Walrand, *J. Mater. Chem.* **2004**, *14*, 191.

[17] A. Getsis, A.-V. Mudring, *Cryst. Res. Technol.* **2008**, *43*, 1187.

[18] V. Tsaryuk, V. Zolin, J. Legendziewicz, *J. Lumin.* **2003**, *102 – 103*, 744; L. D. Carlos, Y. Messaddeq, H. F. Brito, R. A. Sá Ferreira, V. de Zea Bermudez, S. J. L. Ribeiro, *Adv. Mater.* **2000**, *12*, 594; R. A.

Sá Ferreira, L. D. Carlos, R. R. Gonçalves, S. J. L. Ribeiro, V. de Zea Bermudez, *Chem. Mater.* **2001**, *13*, 2991.
[19] M. Fernandes, V. de Zea Bermudez, R. A. Sá Ferreira, L. D. Carlos, A. Charas, J. Morgado, M. M. Silva, M. J. Smith, *Chem. Mater.* **2007**, *19*, 3892.
[20] S. Yanagida, K. Sogabe, Y. Hasegawa, Euro. Pat., EP 1318143, 2003.
[21] G. H. Dieke, 'Spectra and energy levels of rare earth ions in crystals', Interscience Publishers, New York, 1968.

Received May 8, 2009